

# Lawrence Berkeley National Laboratory

## Lawrence Berkeley National Laboratory

**Title**

Some Excitation Functions of Bismuth

**Permalink**

<https://escholarship.org/uc/item/9cv182mb>

**Authors**

Kelly, E.L.  
Segre, E.

**Publication Date**

2008-06-10

UNIVERSITY OF  
CALIFORNIA

*Radiation  
Laboratory*

TWO-WEEK LOAN COPY

*This is a Library Circulating Copy  
which may be borrowed for two weeks.  
For a personal retention copy, call  
Tech. Info. Division, Ext. 5545*

BERKELEY, CALIFORNIA

UCRL 206

Revised

~~Declassification Procedure~~

CLASSIFICATION CANCELLED BY AUTHORITY  
OF THE DISTRICT ENGINEER  
BY THE DECLASSIFICATION COMMITTEE

UNIVERSITY OF CALIFORNIA

**DECLASSIFIED**

Contract No. W-7405-eng-48

PARAMAGNETIC SUSCEPTIBILITIES AND ELECTRONIC STRUCTURES

OF AQUEOUS CATIONS OF ELEMENTS 92 to 95

Jerome J. Howland and Melvin Calvin

December 8, 1948

CAUTION

This document contains information affecting the  
National Defense of the United States.  
Its transmission or the disclosure of its contents  
in any manner to an unauthorized person is prohibit-  
ed and may result in severe criminal penalties under  
applicable Federal Laws.

Berkeley, California

DECLASSIFIED

UCRL 206

Revised

~~CONFIDENTIAL~~

-2-

CLASSIFICATION ON ORDER BY AUTHORITY OF THE DISTRICT ENGINEER  
BY THE DECLASSIFICATION COMMITTEE  
Copy Numbers

DECLASSIFICATION PROCEDURE, Oak Ridge. SERIES A

Declassification Officer  
Publication Officer  
Patent Dept.  
Area Manager, Berkeley  
E. O. Lawrence  
Information Division

1-4  
5  
6-7  
8  
9  
10

INFORMATION DIVISION  
RADIATION LABORATORY  
Univ. of California  
Berkeley, California

DECLASSIFIED

UCRL-206  
(Revised)  
Page 3

December 8, 1948

PARAMAGNETIC SUSCEPTIBILITIES AND ELECTRONIC STRUCTURES

OF AQUEOUS CATIONS OF ELEMENTS 92 TO 95

Jerome J. Howland<sup>(1)</sup> and Melvin Calvin

Radiation Laboratory and Department of Chemistry  
University of California, Berkeley, California

ABSTRACT

Magnetic susceptibilities per gram atomic weight of elements 92 to 95 in most of their oxidation states were measured at 20°C. on 0.1 ml of solution which was 0.005 to 0.09 M in heavy element. The values obtained (all paramagnetic) in e.m.u.  $\times 10^6$  were: U(IV), 3690; Np(VI), 2060; Np(V), 4120; Np(IV), 4000; Pu(IV), 1610; Pu(III), 370; Am(III), 720.

The results could be interpreted only on the basis of electronic configurations  $5f^n$ , even though susceptibilities were generally lower than the theoretical values and lower than experimental values for corresponding lanthanide  $4f^n$  cations. The lower values should be expected as a result of the Stark effect produced by electric fields of anions and of water dipoles. Failure of the Russell-Saunders approximation to the coupling between electrons may account for some of the error in the theoretical calculations. Wider multiplet splitting in the actinides accounts for the fact that the susceptibilities of Pu(III) and Am(III) are many-fold lower than those of Sm(III) and Eu(III) respectively.

December 8, 1948

## PARAMAGNETIC SUSCEPTIBILITIES AND ELECTRONIC STRUCTURES

## OF AQUEOUS CATIONS OF ELEMENTS 92 TO 95

Jerome J. Howland<sup>(1)</sup> and Melvin CalvinRadiation Laboratory and Department of Chemistry  
University of California, Berkeley, California

Chemical and physical properties and theoretical calculations have indicated that elements of about  $Z = 90$  and higher constitute a series in which the 5f orbitals are filled as  $Z$  increases. These heavy elements have been called actinides in analogy to the name lanthanides for the rare earth elements<sup>(2)</sup>. It was of interest to determine whether corresponding aqueous cations of actinide and lanthanide elements have the same outer electronic configurations even though the actinide concept might not require that they be identical.

If an atom has its electrons in question (i.e., those in addition to the inert gas structure) in inner orbitals, the electrons may be electrostatically shielded from neighboring atoms to the extent that the magnetic susceptibility of a solution of such atoms can be deduced from quantum numbers of the ground state of the electronic configuration. Sometimes the converse, deduction of ground state quantum numbers from the susceptibility, will yield a unique answer. The method was successful for the lanthanide tripositive ions which have as outer configurations  $4f^{1-14} 5s^2 5p^6$ .

Susceptibilities of U(IV) and U(III) solutions were reported by Lawrence<sup>(3)</sup>. Solid uranium compounds have been studied by numerous investigators<sup>(4)</sup>. At room temperature the susceptibility of U(IV) solutions and salts approximates the theoretical value derived from the spin magnetic moment of atoms with two unpaired electrons. Since this type of calculation was successful in accounting for the susceptibility of the first row transi-

tion element ions which have partially filled 3d electron orbitals, the observed susceptibility of U(IV) was usually interpreted as evidence for a  $5d^2$  electron configuration. This deduction was inconsistent with the fact that the observed susceptibilities of cations of heavier transition elements (those with partially filled 4d or 5d orbitals) are generally many-fold smaller than the "spin only" calculations, and later studies of general properties of U, Np and Pu made 6d configurations improbable. Hutchison and Elliott<sup>(5)</sup> have interpreted their recent measurements on uranium(IV) susceptibilities on the basis of a  $5f^2$  structure.

Shortly after plutonium became available, the susceptibilities of dilute Pu(VI), Pu(V), Pu(IV), and Pu(III) solutions were measured<sup>(6)</sup> with the expectation that they might closely parallel those of Pr(III) through Sm(III) if the actinide element ions also had  $f^n$  electronic configurations. The measurement of Pu(V) was very crude because of the instability of that state<sup>(7)</sup>. For the other three plutonium oxidation states there was no close agreement with expectations of particular electronic structures. More actinide elements which exist in one or more oxidation states could be used in the present study. Since the alpha activity of the available isotope of curium would rapidly decompose the water of its aqueous solution, experiments with this material were not attempted.

#### Experimental

Magnetic susceptibility measurements were made on 0.1 ml samples which were of the order of 0.01 M in heavy element by use of a bifilar suspension method developed from one described by Theorell<sup>(8)</sup>. A divided glass capillary was suspended as shown in Fig. 1. A solution was in the left compartment; distilled water was in the right. The capillary moved a distance of the order of 0.1 cm when the current through the magnet coils was 40 amps.

(Field strength directly between the pole faces was about 17,000 Gauss.)

The horizontal force,  $F$ , on the capillary very nearly equals  $wD/L$  where  $w$  is the weight of the capillary,  $L$  is the fiber length, and  $D$  is the horizontal displacement which was observed in a microscope equipped with a traveling cross hair. One scale division on the knob corresponds to a distance of  $8 \times 10^{-5}$  cm or to a force of  $6 \times 10^{-7}$  gram if the load is a 0.5 gram capillary.

Each solution was measured several times at magnet coil currents of 20, 30 and 40 amps. in order to establish that susceptibilities were always independent of field strength.

The molar susceptibility,  $\chi$ , of a substance equals  $I_m/H$  where  $I_m$  is the magnetic moment of a gram atomic weight of the bulk material and  $H$  is the magnetic field strength. The total force acting on a long cylinder of solution with cross section  $A$  and whose axis passes through an inhomogeneous field is

$$wD/L = F = \chi \underline{M} A (H_2^2 - H_1^2)/2000 \quad (1)$$

where  $\underline{M}$  is the molar concentration and  $H_1$  and  $H_2$  are the field strengths on the ends of the solution.

Equation (1) would hold only for a homogeneous cylindrical sample; it was used for rough estimation of the field strength  $H_2$  from the displacements of nickel chloride solutions. Susceptibilities of other substances were calculated on the assumption that the displacement was proportional to  $\chi \underline{M}$  if  $w$ ,  $A$ ,  $H_1$  and  $H_2$  were held constant. The displacement was measured for each actinide element solution in the same compartment and at the same magnet coil current ( $\pm 0.2$  amps.) as was done for a standard nickel chloride solution. Correction for diamagnetism of the solvent and of the anions and for non-uniformity of the capillary was made by subtraction of an

experimentally determined displacement. If the molar susceptibility of nickel chloride at 20°C is taken as  $4436 \times 10^{-6}$  c.g.s. e.m.u.<sup>(9)</sup>, then for any cation

$$\chi = 4436 \times 10^{-6} D' \frac{M_{\text{NiCl}_2}}{M D'_{\text{NiCl}_2}} \quad (2)$$

where D' is the displacement after application of the correction.

The U(IV) solution was prepared by dissolution of weighed, distilled  $\text{UCl}_4$  in oxygen-free hydrochloric acid solution. The last step in the preparation of the neptunium, plutonium, and americium solutions was dissolution of a hydroxide which had been precipitated with ammonium hydroxide. The plutonium concentrations were based on a weighing. The neptunium and americium solutions were assayed by measurement of the rate of alpha particle emission of a small aliquot. The specific activities in counts/min./ $\mu\text{g}$ . were taken as 790 for  $\text{Np}^{(10)}$  and  $3.36 \times 10^6$  for  $\text{Am}^{(11)}$  if a thin sample is mounted on platinum and a counter geometry of "50%" is used<sup>(12)</sup>. These values are said to be probably better than  $\pm 5\%$ . If better specific activities are reported at a later date, the magnetic susceptibilities should be corrected proportionately. The quantity of neptunium or plutonium which was not in the desired oxidation state was shown to be less than 1% by measurement of the characteristic optical absorption maxima<sup>(13)</sup> on a Beckman spectrophotometer.

The 0.03920 M nickel chloride solution which served as magnetic standard was prepared by dissolution of 0.2301 g. of nickel rod (Johnson Matthey and Co., 99.97% Ni) in 5 ml of refluxing 10 M HCl. After the solution had been diluted to 100.0 ml, the excess HCl concentration was found to be 0.360 M.

Although the measured displacements were reproducible to about one scale division, the uncertainty in the molar susceptibilities is about 2% or  $30 \times 10^{-6}$  units, whichever is larger, because of the inaccuracy in determination of actinide element concentration and because of the presence in

the solutions of an unknown amount of diamagnetic ammonium ion. The large negative displacements listed for some examples of solvent only in the rear compartment are due to non-uniformity of the glass capillary. These large negative subtractions do not increase the percent error if the gross displacement of the actinide solution is positive.

### Results and Interpretation

Some typical data are given in Table I. In Fig. 2 experimental  $\chi$  of the actinide element cations are compared with simple theoretical  $\chi_j$  for the assumed ground quantum states of the electronic configurations  $5f^n$  and  $5f^{n-1}6d$ . The experimental  $\chi$  follow the  $\chi_j$  for configurations  $f^n$  to a significant degree, though not as closely as had been found for most of the lanthanide cations<sup>(14)</sup>. The susceptibility of Am(III) is much higher than the theoretical value of zero, but that is also true of the corresponding lanthanide ion, Eu(III). It will be discussed in a later section of this paper. The susceptibilities of the cations are, of course, dependent upon the anion to a secondary degree<sup>(3)</sup>.

The ground states of the cations Np(VI), Np(V), Np(IV), Pu(IV), Pu(III), and Am(III) were concluded to be those on which the theoretical curve B was based, i.e.,  $^2F_{5/2}$ ,  $^3H_4$ ,  $^4I_{9/2}$ ,  $^5I_4$ ,  $^6H_{5/2}$ , and  $^7F_0$  respectively as  $n$  is 1 through 6.

While the atomic quantum numbers of a state may be those which are expected for a definite configuration,  $f^n$ , the state can belong partly to another configuration of the same parity<sup>(16)</sup>. Susceptibility measurements can show only that the ground state has certain L, S, and J quantum numbers; identification of the state with a configuration is a useful approximate concept. To the extent that quantum states of complicated atoms can be attributed to a single electronic configuration, the known aqueous cations of uranium and higher elements must have as the outer part of their ground

configurations,  $5f^n 6s^2 6p^6$  ( $n$  5f electrons which are more or less inside the configuration for the inert gas element 86).

#### Approximate Nature of Theoretical Calculations

The factors which account for the limited accuracy of our theoretical calculations should be mentioned. Quantum statistically the susceptibility is given by the relation<sup>(15)</sup>

$$\chi = \frac{I_m}{H} = \frac{N_0}{H} \frac{\sum W_i / \exp(-W_i/kT)}{\sum \exp(-W_i/kT)} \quad (3)$$

where  $N_0$  is Avogadro's number and the summations are over all quantum states of energies  $W_i$ . If the energy levels are simply those resulting from the Zeeman splitting of an isolated (on the energy scale) state of a free atom, their energies might be assumed to be

$$W_i - W_i^0 = H g \beta M \quad (4)$$

where  $\beta = eh/4\pi mc$  and  $M = J, J-1, \dots, -J$ . Since  $2H g \beta J \ll kT$ <sup>(4)</sup> equation (3) yields

$$\chi_J = N g^2 \beta^2 J(J+1)/3kT \quad (5)$$

If the angular momenta of the several electrons are coupled according to the Russell-Saunders scheme (LS coupling)

$$g = [3J(J+1) + S(S+1) - L(L+1)]/2J(J+1) \quad (6)$$

Equations (5) and (6) were used to calculate the theoretical points of Fig. 2. The ground state of a configuration was assumed by application of Hund's rules. The limited agreement of theoretical and experimental susceptibilities indicates that each paramagnetic atom interacts with other surrounding atoms as well as with the external magnetic field. Since most of the surrounding atoms are diamagnetic, the interaction is probably electrostatic in nature.

Penny and Schlapp attempted to calculate the effect of crystal electric

fields on the magnetic susceptibility of iron group compounds and rare earth salts<sup>(18,19)</sup>. Qualitatively it is a Stark splitting which is of the order of  $kT$  whereas the Zeeman splitting is small compared to  $kT$ . Although the calculations are not perfected<sup>(20)</sup>, it is clear that the summation (3) can be much smaller than its evaluation by equation (5). Similarly in solutions the electric fields of neighbor anions and water dipoles will lower the magnetic susceptibility of an actinide element cation compared to its corresponding lanthanide ion since the 5f electrons of the former should be outside the valence shell more often than are the 4f electrons in the latter. Since Np(VI) is essentially a one-electron case, the complications to be mentioned later cannot be important, and the 25% lowering of the susceptibility from the theoretical  $\chi_J$  must be due to the Stark splitting. It may be assumed that the Stark effect is the most important single complication tending to lower the susceptibility of all the actinide element cations.

Ground quantum states of the  $4f^n$  configurations were deduced by Hund<sup>(14)</sup> from rules which are correct for atoms of small  $Z$  in which case it is a good approximation to derive atomic states from the states of individual electrons by means of the LS or Russell-Saunders coupling model (vanishingly weak spin-orbit interaction). In the spectra of gaseous uranium<sup>(21,22)</sup> the multiplet splitting is wider than the separation of the centers of gravity of LS states. By definition this is strong spin-orbit interaction. The experimental  $g$ 's of low lying states of the  $5f^3 6d 7s^2$  configuration of uranium are fairly close to  $g_{LS}$ , however.

It is interesting to see what happens to the energy levels as the spin-orbit interaction increases and the interelectronic interaction approaches the limiting case of  $jj$  coupling. Column 2 of Table III lists some states which should lie very low in the configurations  $5f^{1-6}$ . The

state listed first lies deepest according to Hund's rules. For  $5f^2$ ,  $5f^3$ , and  $5f^4$  the state listed second was selected because it belongs both to the next group according to LS coupling and to the lowest group of jj coupling states. The ground state of  $5f^5$  or of  $5f^6$  becomes more isolated as jj coupling is approached. In the case of  $5f^6$  the two lowest multiplets of  $^7F$  were selected because the spacing between  $J = 0$  and  $J = 1$  would be only  $1/21$  of the total multiplet splitting according to the Landé interval rule. The relative importance of the probably second lowest states is not known at the present time except that  $^7F_1$  must be significantly populated in Am(III) at  $20^\circ\text{C}$ .

Theoretical  $\chi_J$ 's for each ground state of the  $5f^n$  configurations were calculated for both coupling approximations, and the two results diverge as  $n$  increases from 2 to 5. Since the two  $\chi_J$ 's differ directly as  $g_{LS}^2$  and  $g_{jj}^2$  differ, the experimental  $\chi$  of Pu(III), the example of  $5f^5\ ^6H_{5/2}$ , shows unambiguously that  $g$  is much nearer to  $g_{LS}$  than to  $g_{jj}$ . This is consistent with previously mentioned results for the gaseous uranium atom.

Equation (5) depends on the validity of equation (4) for the Zeeman splitting. For each low energy state of Sm(III) and Eu(III) it was necessary<sup>(23)</sup> to use a more complete equation for  $\chi_J$  which had been derived by Van Vleck<sup>(15)</sup> from considerations equivalent to taking the Zeeman splitting to the second order terms in  $H$ . He obtained equation (5) with the following added on the right:

$$\frac{N\beta^2}{6(2J+1)} \left\{ \frac{f(J)}{h\nu(J-1; J)} + \frac{f(J+1)}{h\nu(J+1; J)} \right\} \quad (5a)$$

where  $f(J) = [(S+L+1)^2 - J^2] [J^2 - (S-L)^2]/J$

For sufficiently large  $h\nu$ 's this addition is negligible except that when  $S$  and  $L$  are large and  $J$  is small the  $f/h\nu$  terms are extremely large. In the examples

Pu(III) and Am(III) the susceptibilities are greater than theoretical  $\chi_J$ 's for  $^6H_{5/2}$  and  $^7F_0$  as obtained with equation (5). The  $f/h\nu$  terms must be significant for low lying states of both cations. While the  $^7F_1$  state must be well populated in Am(III), it is much less so than in Eu(III) where the multiplet splitting is narrower. Thus the same discrepancies with simplest theory that were important in Sm(III) and in Eu(III) can be detected in Pu(III) and Am(III). The analogy is shown clearly in Fig. 3 where experimental susceptibilities of lanthanide and actinide element cations are compared directly.

#### Acknowledgement

The neptunium and americium were available for this study only through the work of T. J. LaChapelle, L. B. Magnusson, L. B. Asprey, and B. B. Cunningham, who had isolated these materials in very pure form. Many others contributed, of course, to the production of these special materials. (24)

This paper is based on work performed under the auspices of the Atomic Energy Commission at the Radiation Laboratory, University of California.

Table I  
Typical Data; Displacements of Capillary  
for 40 Ampere Magnet Coil Current

Material in Rear Compart.	Displacement		Suscept. e.m.u. x 10 <sup>6</sup>
	D	D'	
0.36 M HCl	-030		
0.0392 M NiCl <sub>2</sub> in 0.36 M HCl	+991	1021	4436 <sup>a</sup>
0.50 M HCl	-030		
0.0600 M Pu(III) in 0.5 M Cl <sup>-</sup>	+099	129	370
0.50 M H <sub>2</sub> SO <sub>4</sub>	-089		
0.0507 M Pu <sup>2+</sup> (IV) in 0.5 M HSO <sub>4</sub> <sup>-</sup>	+389	478	1610

<sup>a</sup>Magnetic standard, ref. 9.

Table II  
Molar Susceptibilities of Actinide Element Cations  
at 20°C in Aqueous Solution

Cation in Solution	Anion in Solution	Cation Suscept. e.m.u. $\times 10^6$
U(IV)	0.5 <u>M</u> Cl <sup>-</sup>	3690 <sup>a</sup>
Np(VI)	0.5 <u>M</u> HSO <sub>4</sub> <sup>-</sup>	2060
Np(V)	0.2 <u>M</u> Cl <sup>-</sup>	4120 <sup>a</sup>
Np(IV)	0.2 <u>M</u> HSO <sub>4</sub> <sup>-</sup>	4000 <sup>b</sup>
Pu(IV)	0.5 <u>M</u> HSO <sub>4</sub> <sup>-</sup>	1610
Pu(III)	0.5 <u>M</u> Cl <sup>-</sup>	370
Am(III)	0.5 <u>M</u> NO <sub>3</sub> <sup>-</sup>	720

<sup>a</sup>For Pu(VI) (same number of electrons as U(IV) and Np(V)) susceptibility is  $3540 \times 10^{-6}$ , ref. 6.

<sup>b</sup>For U(III) (same number of electrons as Np(IV)), susceptibility is  $4340 \times 10^{-6}$ , ref. 3.

Table III  
Theoretical Susceptibilities of Possible Low Energy  
States of Actinide Ions

Assumed Elect. Config.	Possible Low Energy States	Theor. $\chi_J$ 's LS Coupl. 20°C	Theor. $\chi_J$ 's jj Coupl. 20° C
$5f^1$	$^2F_{5/2}$	2730	2730
$5f^2$	$^3H_4; ^3F_2$	5420; 1130	6210; 1870
$5f^3$	$^4I_{9/2}; ^4G_{5/2}$	5540; 1210	7680; 2730
$5f^4$	$^5I_4; ^5G_2$	3040; 280	6210; 1870
$5f^5$	$^6H_{5/2}$	300	2730
$5f^6$	$^7F_0; ^7F_1$	0; 1900	0; 1900
$5f^6d$	$^3H_4; ^3G_3$	5420; 2860	
$5f^2 6d$	$^4K_{11/2}; ^4I_{9/2}$	8950; 5540	
$5f^3 6d$	$^5L_6; ^5K_5$	9070; 5670	
$5f^4 6d$	$^6L_{11/2}; ^6K_{9/2}$	5730; 3130	
$5f^5 6d$	$^7K_4; ^7I_3$	1350; 320	

Fig. 1.--Apparatus for measurement of magnetic susceptibility: A, glass fibers, 0.005 x 140 cm; B, glass capillary, 0.2 x 16 cm; C, magnet pole faces, 2.5 cm diam.; D, mirror and microscope; E, magnet pole pieces, 15 cm diam.

Fig. 2.--Comparison at 20°C of magnetic susceptibilities of actinide element cations with theoretical susceptibilities: A, experimental; B, theoretical for ground states of  $5f^n$ ; C, theoretical for ground states of  $5f^{n-1}6d$ .

Fig. 3.--Comparison of experimental magnetic susceptibilities of lanthanide and actinide element cations at 20°C. The values for the lanthanides were calculated from some of the "effective magnetic moments" compiled by Yost, Russell and Garner (The Rare Earth Elements and Their Compounds, Wiley, New York, 1947, p. 14.). The point for  $61(III)$  is from the theoretical calculation by Van Vleck and Frank (See ref. 23).

### References

1. Now at Brookhaven National Laboratory, Upton, L. I., New York.
2. Some of the properties of the recently discovered heavy transition elements were reviewed and the name actinides was suggested by Seaborg, G. T., Chem. and Eng. News 23, 2190 (1945); Science 104, 379 (1946). Zachariasen, W. H., Phys. Rev. 73, 1104 (1948) used the name actinide for the +3 ions only, thorides for +4 ions, etc., in reporting his x-ray diffraction studies which showed that the solid compounds have the crystal structures and ionic radii consistent with assumption of 5f electronic configurations. We use Seaborg's nomenclature.
3. Lawrence, R. W., J. Am. Chem. Soc. 56, 776 (1934).
4. See reference 5 for keys to this literature.
5. Hutchison, C. A., Jr., and N. Elliott, J. Chem. Phys. 16, 920 (1948).
6. Calvin, M., Plutonium Project Report CK-2411 (1944). Calvin, M., M. Kasha and G. Sheline, AECD-2002 (1948).
7. Connick, R. E., M. Kasha, W. H. McVey, and G. Sheline, "The +5 Oxidation State of Plutonium", Plutonium Project Record, Vol. 14B, No. 3.15 (to be published).
8. Theorell, H., Arkiv Kemi, Mineral., Geol. 16A, No. 1 (1943). Our apparatus was essentially the one used but not described by Lewis, G. N., and M. Calvin, J. Am. Chem. Soc. 67, 1232 (1945).
9. Nettleton, H. R., and S. Sugden, Proc. Roy. Soc. (London) A173, 313 (1939).
10. Magnusson, L. B., and T. J. LaChapelle, "The First Isolation of Element 93 in Pure Compounds and a Determination of the Half-Life of  $\text{Np}^{237}$ ", J. Am. Chem. Soc. (to be published).
11. Cunningham, B. B., Plutonium Project Report CC-3876, Sect. 2.2 (1948).
12. About 52% of the disintegrations are counted. Cunningham, B. B., A. Ghiorso, and J. C. Hindman, "Back-Scattering of  $\text{Pu}^{239}$  Alpha Particles from Platinum", Plutonium Project Record, Vol. 14B, No. 16.3 (to be published).
13. Hindman, J. C., and D. P. Ames, "Absorption Spectra of Ionic Species of Plutonium", Plutonium Project Record, Vol. 14B, No. 4.1; Hindman, J. C., L. B. Magnusson and T. J. LaChapelle, "Chemistry of Element 93, III. Absorption Spectrum Studies of Aqueous Ions of Neptunium", Ibid., No. 15.2.
14. Hund, F., Z. Physik 33, 855 (1925).
15. Van Vleck, J. H., Phys. Rev. 31, 587 (1928).

16. Condon, E. U., Ibid. 36, 1121 (1930).
17. The small contribution to susceptibility from the magnetic moment induced by the applied field was not added to the theoretical  $\chi_J$ 's. It would be only about  $-50 \times 10^{-6}$  for monatomic ions represented by  $\text{Pu}^{+3}$  and  $\text{Am}^{+3}$  and possibly as much as  $+50 \times 10^{-6}$  for molecular types such as  $\text{NpO}_2^+$  and  $\text{NpO}_2^{++}$ .
18. Penny, W. G., and R. Schlapp, Phys. Rev. 41, 194 (1932); Schlapp and Penny, Ibid. 42, 667 (1932). These authors pointed out the absence of any fundamental significance of the empirical Weiss-Curie relation,  $\chi = C/(T + \Delta)$ . Many investigators have calculated "effective atomic magnetic moments" as  $\mu_{\text{eff}} = (C k/N)^{1/2}$  and compared this "experimental" moment with  $\mu = g\beta [J(J + 1)]^{1/2}$ . These  $\mu_{\text{eff}}$  can have no more meaning than C, which sometimes approaches  $N\mu^2/3k$  when  $\Delta$  is nearly zero. It seems preferable to present all results as susceptibilities and then compare theoretical values with the directly observed quantities even though the discrepancies seem twice as great when the device of square root extraction is not used.
19. Frank, A., Ibid. 48, 765 (1935).
20. For more recent discussions see Penny, W. G., and G. J. Kynch, Proc. Roy. Soc. (London) A170, 112 (1939) and Broer, L. J. F., Physica 12, 642 (1946).
21. Kiess, C. C., C. J. Humphreys and D. D. Laun, J. Optical Soc. Am. 36, 357 (1946).
22. Schuurmans, Ph., Physica 11, 475 (1946); Schuurmans, Ph., J. C. van den Bosch and N. Dijkwel, Ibid. 13, 117 (1947).
23. Van Vleck, J. H., and A. Frank, Phys. Rev. 34, 1494, 1625 (1929).
24. See forthcoming Plutonium Project Record, Volume 14A and 14B.

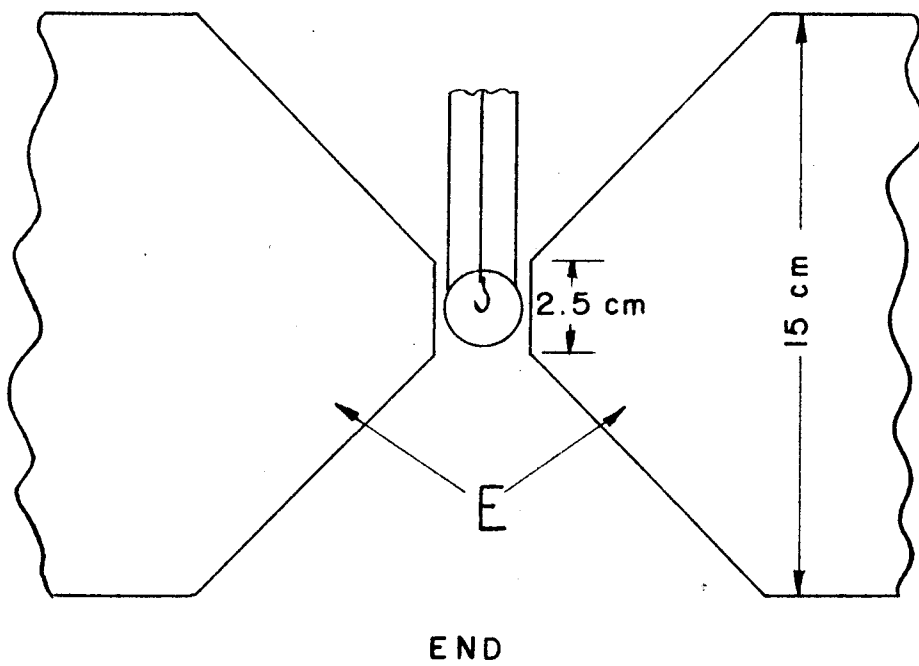
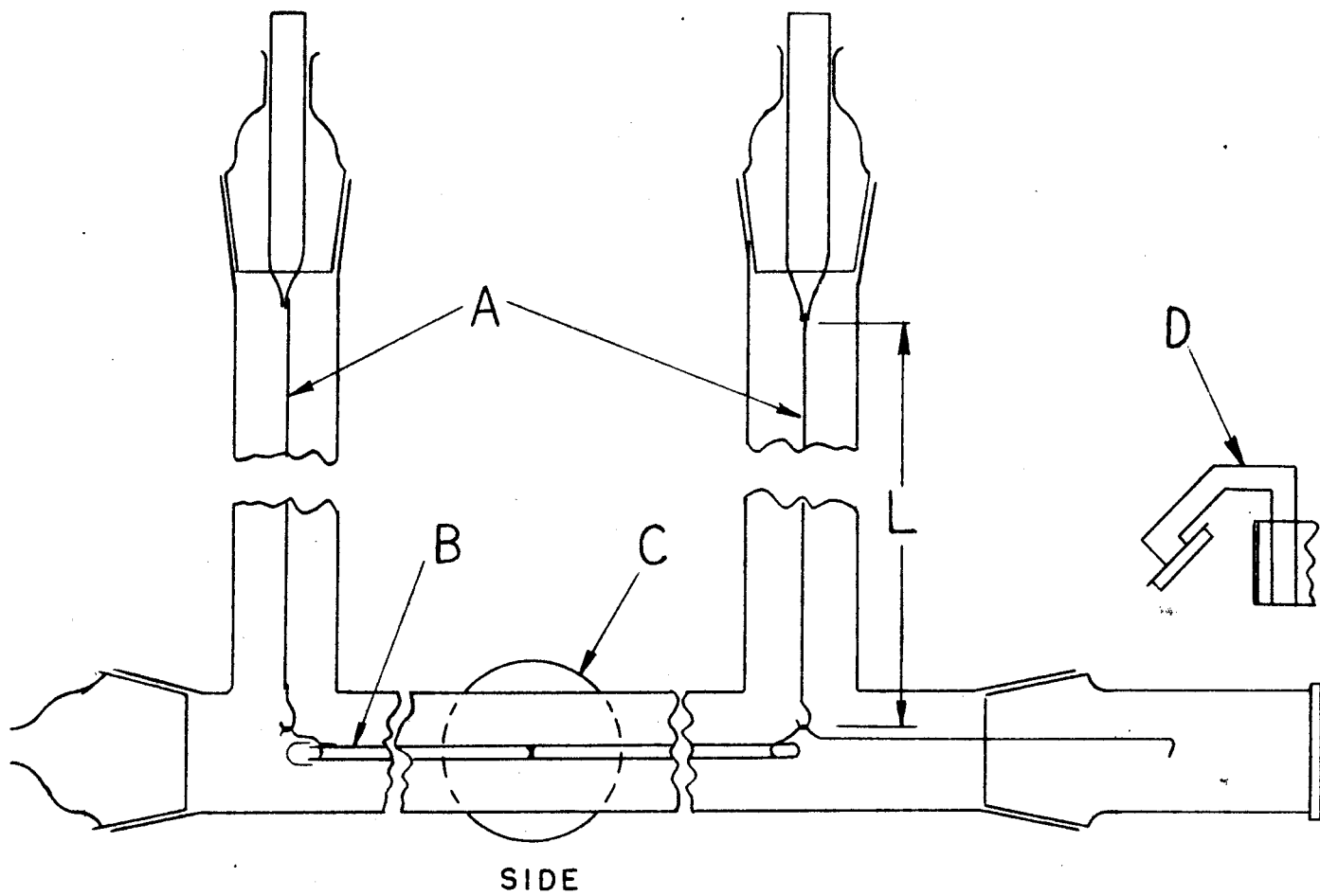
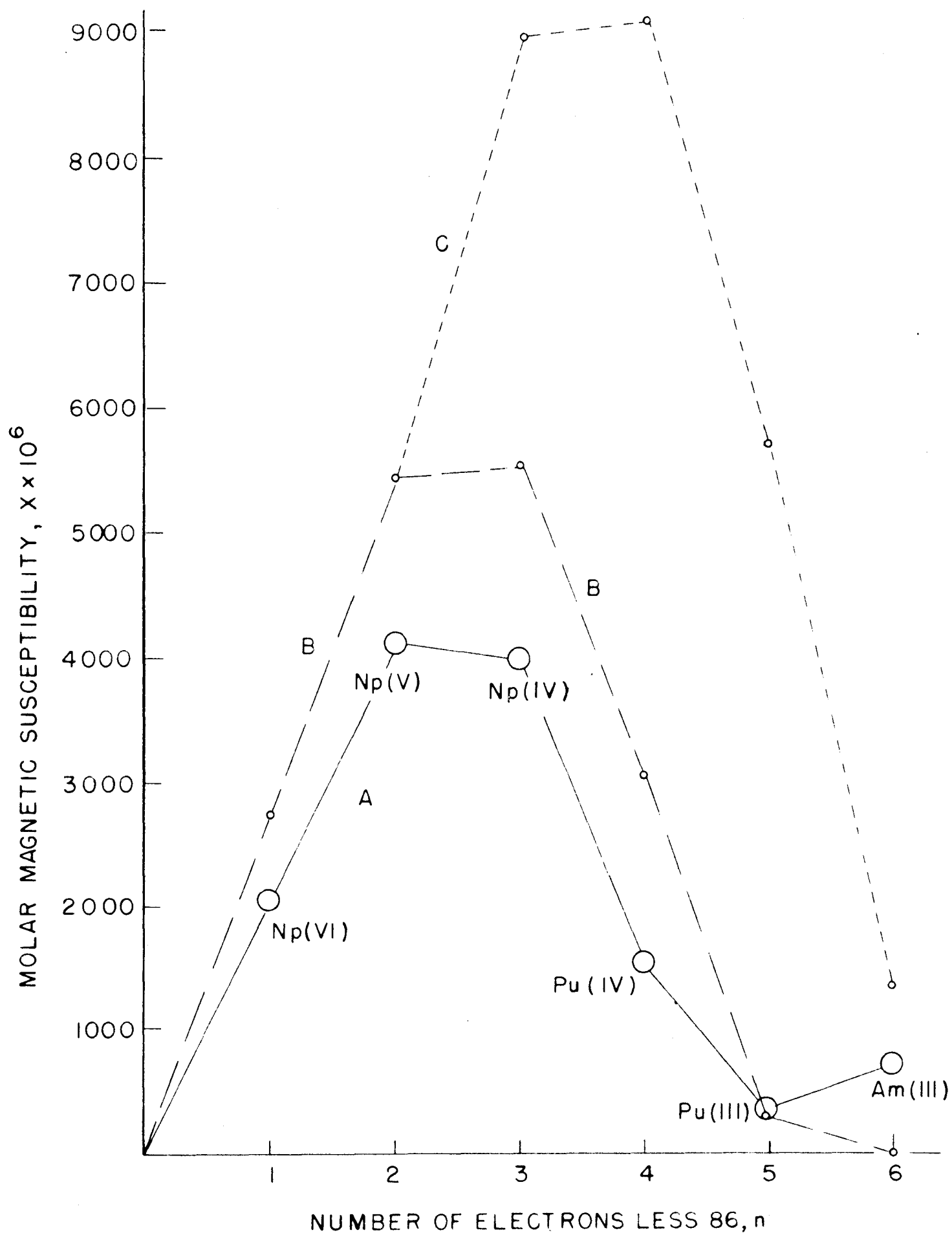


FIG. 1



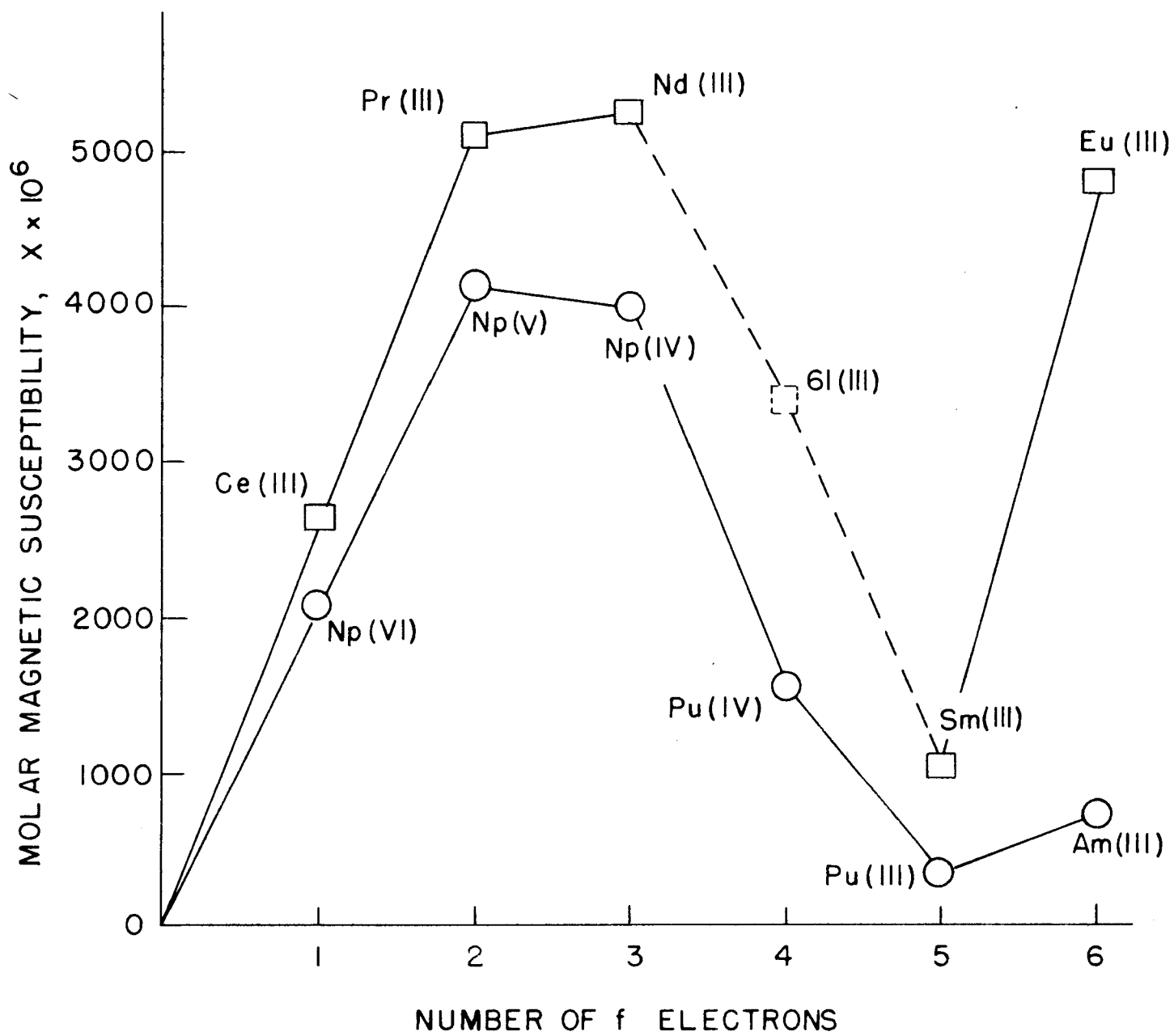


FIG. 3

UNIVERSITY OF  
CALIFORNIA

*Radiation  
Laboratory*

FOR REFERENCE

NOT TO BE TAKEN FROM THIS ROOM

BERKELEY, CALIFORNIA

**Special Review of  
Declassified Reports**

Authorized by USDOE JK Bratton

Unclassified TWX P182206Z May 79

UCRL-207 1948

**REPORT PROPERLY DECLASSIFIED**

*HL Kreen*

Authorized Derivative Classifier

*Larry Boken*

*3-25-80*

Date

Copy 1

UNIVERSITY OF CALIFORNIA

Radiation Laboratory

Contract No. W-7405-eng-48

~~CONFIDENTIAL~~  
CLASSIFICATION DECLASSIFIED BY AUTHORITY  
OF THE  
BY THE DECLASSIFICATION COMMITTEE

SOME EXCITATION FUNCTIONS OF BISMUTH

E. L. Kelly and E. Segrè

November 10, 1948

**UNCLASSIFIED**

Berkeley, California

## Physics-General

-2-

Standard DistributionCopy Nos.

Argonne National Laboratory	1-8
Armed Forces Special Weapons Project	9
Atomic Energy Commission, Washington	10-11
Battelle Memorial Institute	12
Brookhaven National Laboratory	13-20
Bureau of Ships	21-
Carbide & Carbon Chemicals Corp. (K-25 Plant)	22-25
Carbide & Carbon Chemicals Corp. (Y-12 Plant)	26-29
Columbia University (Dunning)	30
General Electric Company, Richland	31-34
Hanford Operations Office	35
Iowa State College	36
Knolls Atomic Power Laboratory	37-40
Los Alamos	41-43
Mound Laboratory	44-45
National Bureau of Standards	46-47
Naval Radiological Defense Laboratory	48
NEPA Project	49
New York Operations Office	50-51
North American Aviation, Inc.	52
Oak Ridge National Laboratory	53-60
Patent Advisor, Washington	61
Sandia Base	62-63
Technical Information Division, OROO	64-78
UCLA Medical Research Laboratory (Warren)	79
University of California Radiation Laboratory	80-84
University of Rochester	85-86
Declassification Procedure	
Declassification Officer	87-90
Publication Officer	91
Patent Department	92-93
E. O. Lawrence	94
Area Manager	95
Information Division	96

Total

96

Information Division  
Radiation Laboratory  
University of California  
Berkeley, California

## SOLE EXCITATION FUNCTIONS OF BISMUTH

E. L. Kelly and E. Segrè

Radiation Laboratory, Department of Physics  
University of California, Berkeley, California

November 10, 1948

Bismuth has long been a favorite element for excitation function work. This is due in part to the fact that bismuth has a single stable isotope, is abundant, and is easily evaporated to form thin uniform films. Also many of the products of bismuth bombarded with deuterons or alphas are alpha-active which is convenient for determination of absolute counting rates. Early investigators<sup>(1)(2)(3)</sup> in this field had available deuterons up to 9 Mev energy. In later work deuterons up to 14 Mev<sup>(4)</sup> and alphas up to 28 Mev energy<sup>(5)</sup> were used. In spite of the excellence of the work that already had been done in bismuth the availability of the 19 Mev deuteron beam and the 38 Mev alpha beam of the 60" Crocker Radiation Laboratory cyclotron made further work seem worth while. The method used in the present work is the well known stacked foil technique with some improvement in the definition of the energy and the measurement of the beam current. A stack of aluminum foils, each having a thin film of evaporated bismuth on one side, was exposed to the collimated beam of the Crocker 60" cyclotron. The stack was not thick enough to stop the beam which was caught in a Faraday cup, amplified, and fed into a recording milliammeter. The mean range of the cyclotron beam was found by determining the amount of aluminum absorber required to reduce the beam intensity to one half. The activity induced in the bismuth films was counted by means of a parallel plate ionization chamber. Fig. 1 gives a schematic diagram of the apparatus used for the bombardments. Tables I and II and Figs. 4 and 5 give the final results, i.e., the cross sections for the various processes as a function of the energy of the bombarding deuteron or alpha particle.

### Experimental Details

The aluminum foil used as backing for the evaporated bismuth and for the energy determination absorbers, was punched on a die whose area was accurately measured. The dimensions of several foils were also measured with a traveling microscope. The areas of the various foils agreed to better than 3 parts in a thousand. Each backing foil, which was 0.001 inches thick, was thoroughly cleaned in  $\text{CCl}_4$  and absolute alcohol, and weighed on an assay balance to the closest 0.01 mg. Next, the foils were placed in a high vacuum chamber and bismuth evaporated onto them to the desired thickness. (Most runs were made with 1 to 1.5  $\text{mg}/\text{cm}^2$  of bismuth). The foils were then reweighed and the thickness of bismuth determined with an estimated accuracy of 1 part in 200 or better.

The raw beam of the 60" Crocker cyclotron had enough inhomogeneity in energy so that a better definition of the energy was required. This was obtained with a collimation system which consisted of the deflector channel of the cyclotron and the 1/8 inch slit shown in Fig. 1. Due to the magnetic field of the cyclotron this collimation system served as a velocity selector producing a beam of very homogeneous energy. Tests of energy versus deflector voltage showed a dependence of 0.04 Mev per kilovolt on the deflector. In practice the deflector voltage was held constant to 2 kilovolts for the entire run. Since this collimation reduced the primary beam intensity by a factor of approximately one hundred (from  $10^{-5}$  -  $10^{-6}$  to  $10^{-7}$  -  $10^{-8}$  amp) a sensitive beam current integrator was necessary. The current to the Faraday cup of Fig. 1 ( $10^{-7}$  to  $10^{-8}$  amp) was amplified to 1 milliampere by a modified version of the current amplifier described by Vance<sup>(6)</sup>, and recorded on an Esterline Angus recording milliammeter. The integrated beam current was found by planimentering the area under the trace. The trace of each run was planimentered by two people and the agreement was 1 part in 200 or better. Allowance was made for the peculiar form of the Esterline Angus trace.

The range of the collimated beam was determined in a manner similar to that described by Wilson<sup>(7)</sup>. The foil wheel shown in Fig. 1 contained aluminum absorbers differing in thickness by approximately 1  $\text{mg}/\text{cm}^2$ . Each of these absorbers in turn was

placed in the path of the beam while the amount of beam current stopped and the amount transmitted were determined simultaneously by current amplifiers<sup>(6)</sup>. This gave the fraction of the total beam current transmitted for various thicknesses of aluminum absorber. From this data the mean beam range was at once determined. The position of the foil wheel could be changed by remote control and since the stacked bismuth foils were contained in the wheel it was possible to determine the beam range, bombard the stacked bismuth foils, and redetermine the beam range without turning off the cyclotron. The range data for a typical run are plotted in Fig. 2. It will be noted that there was little change in the beam range during the run. The straggling of 1.1 percent compares favorably with the theoretical minimum of 0.9 percent given by Livingston and Bethe<sup>(8)</sup>. The range in aluminum was converted to energy using the table of Smith<sup>(9)</sup>.

The activity induced in the bismuth films was followed by counting each sample in a parallel plate ionization chamber having a depth of 1.5 cm. and filled with argon at a pressure of 1.7 atmospheres. The pulses from electron collection in the chamber were fed into a pre-amplifier and then into an amplifier whose time of rise was 0.2 microseconds. The amplified pulses were discriminated and counted on a 256 scaling circuit and mechanical register. The counter was checked against a standard alpha-particle source (a thin uranium sample electro deposited on platinum) at the beginning and end of each counting period, and was found to remain constant to one percent over the entire period of 2 years during which these studies were made. The background was 1 to 2 counts per minute. The counting rate of the uranium alpha standard as a function of discriminator bias is shown in Fig. 3. The counting efficiency at the operating bias of 14 has been taken to be 0.50. This round number takes into account the absorption in the sample itself and the back scattering from support.

The possibility of error in the beam current measurements due to gas ionization or secondary electron emission was investigated. The space around the Faraday cup and the foil wheel was connected to the cyclotron tank during normal operation as shown in

Fig. 1. Since the pumping speed of the opening of the defining slits was small, a leak in this region could cause a substantial increase in pressure with a resulting increase in gas ionization along the path of the beam between the slits and the Faraday cup. Any selective collection of these gas ions would of course introduce an error. To test this effect, the pressure in the region of the Faraday cup was gradually increased until the cyclotron tank pressure showed a 50 percent increase. At this juncture the pressure in the region of the Faraday cup was approximately 10 microns of mercury but no evidence of gas ionization was observed on the beam current meters. Since in normal operation no observable change in cyclotron tank pressure was produced by our apparatus this source of error must be ruled out. The effect of possible secondary emission of electrons is also ruled out. The fringing magnetic field of the cyclotron is 2500 gauss in the region where the Faraday cup was located. The resulting curvature in the path of any secondary electron formed by the beam striking the bottom of the Faraday cup would be more than sufficient to prevent the escape of the electron.

#### Bi ( $\alpha, 2n$ ) and Bi ( $\alpha, 3n$ ) Excitation Functions

At bombarding alpha energies below 29 Mev the only alpha-particle activity observed in the bombarded bismuth was that of At<sup>211</sup>, which has a half-life of 7.5 hr. At higher bombarding alpha energies another alpha-activity was observed after the 7.5 hr activity had died out. This was found to be due to Po<sup>210</sup>. No other alpha-activity was detected. This made the separation of activities extremely simple. An alpha count 5 or 6 days after bombardment gave only the Po<sup>210</sup> activity; correcting this for decay and subtracting from a count made soon after bombardment we obtained the activity due to At<sup>211</sup>, which could then easily be extrapolated back to the time of the end of bombardment. This method of separating the activities was quick and accurate\*. The question immediately arose, however, as to the origin of the Po<sup>210</sup>. Careful investigation, which will be discussed in detail later, showed that the Po<sup>210</sup> came from the Bi( $\alpha, 3n$ ) reaction producing

\*This method neglects the 8.3 hr half-life for formation of the Po<sup>210</sup> mentioned below, but the resulting error introduced was found to be negligible in all cases.

$\text{At}^{210}$  which in turn decays to  $\text{Po}^{210}$  by orbital electron capture, with a half life of 8.3 hr. Thus the  $\text{At}^{210}$  which had no alpha-activity decayed to an alpha emitter which was readily counted on an absolute scale. The results of three runs were analyzed in this way and reduced to absolute cross section versus energy of the bombarding alphas. One run was made with bismuth films of  $0.3 \text{ mg cm}^{-2}$ , one with  $1.5 \text{ mg cm}^{-2}$ , and one with  $2.0 \text{ mg cm}^{-2}$ . When the results of these runs were first compared to a dispersion of a few percent was found, which was felt to be outside the experimental error. After thorough checking, this dispersion was tentatively laid to the inaccuracy in the stopping power ratio of bismuth to aluminum, which had been extrapolated from the value for gold given by Bethe<sup>(8)</sup>. A subsequent experimental determination of this stopping power ratio removed the apparent dispersion. The results of the three runs are shown in Fig. 4 and Table I.

#### Bi (d,p), Bi (d,n), and Bi (d,3n) Excitation Functions

The activities resulting from deuterons on bismuth are more difficult to separate than those from alphas on bismuth. Early work has established the production of RaE and  $\text{Po}^{210}$  from the Bi (d,p) and Bi (d,n) reactions. Recent work<sup>(10)</sup> shows rather conclusively that the Bi (d,2n) reaction is not observed and that the only alpha-activity at these energies, other than that due to the Bi (d,n) and Bi (d,p) reactions, is due to the Bi (d,3n) reaction which results in  $\text{Po}^{208}$  with a half-life of about 3 years. This is in agreement with the results of two deuteron on bismuth runs made by the authors.

For the separation of the  $\text{Po}^{210}$  with a 140 day half-life, the  $\text{Po}^{208}$  with a 3 year half-life, and the RaE, which goes by 5-day- $\beta$ -decay to  $\text{Po}^{210}$ , the following procedure was adopted\*. Each sample was alpha-counted as soon as possible after bombardment and daily for a week; each sample was counted again after 2 months when all of the 5 day RaE had decayed into  $\text{Po}^{210}$ , and thereafter once every 3 months for a year. In order to determine the  $\text{Po}^{208}$  half-life, ten samples were analyzed by trial and error into 140 day

\*It is not practical to use the difference in energy between the alphas of  $\text{Po}^{208}$  and  $\text{Po}^{210}$  to distinguish between the two because the difference is too small (5.298-5.14 Mev).

$\text{Po}^{210}$  and  $\text{Po}^{208}$ , such that when the  $\text{Po}^{210}$  activity was subtracted, the resulting activity fell on a straight line on semilog paper. The slope of this line gave the  $\text{Po}^{208}$  half-life. The result was  $3.0 \pm 0.2$  years where the error given is based on internal consistency only. Each bombarded sample was then analyzed by the same method except that the resulting activity after  $\text{Po}^{210}$  subtraction was required to fit a straight line with a slope corresponding to a half-life of 3.0 years. This yielded the  $\text{Po}^{208}$  activity, which was extrapolated back to the time of the end of bombardment, and the total  $\text{Po}^{210}$  activity which was also extrapolated back to the time of the end of bombardment. Subtracting the extrapolated  $\text{Po}^{208}$  from the activity measured immediately after bombardment gave the  $\text{Po}^{210}$  due to the  $\text{Bi} (d,n)$  reaction. From the extrapolated total  $\text{Po}^{210}$  activity and the  $\text{Po}^{210}$  activity due to the  $\text{Bi} (d,n)$  reaction, the amount of RaE was found. The amount of RaE was also found by the growth of the total alpha-activity in the first week after bombardment. These two determinations of RaE agreed within one percent. The results of two runs of deuterons on bismuth reduced to absolute cross section versus energy of the bombarding deuterons are shown in Fig. 5 and Table II.

#### Astatine<sup>210</sup>

Bismuth bombarded with alpha particles of 37 Mev energy yields the 7.5 hr alpha-activity of  $\text{At}^{211}$ , and the 140 day alpha-activity of  $\text{Po}^{210}$ , as was mentioned above; in addition, there is an easily distinguishable gamma-ray activity. The  $\text{Po}^{210}$  alpha-activity was found to decrease with decreasing energy of the bombarding alphas, disappearing with alpha energies below 29 Mev (see Fig. 4). The gamma-activity likewise disappeared with bombarding alpha energies below 29 Mev. The gamma-activity was found to follow the  $\text{At}^{211}$  alpha-activity quantitatively through a chemical separation and through a vacuum distillation over to a cold platinum plate<sup>(11)</sup>. In the separated astatine fraction  $\text{Po}^{210}$  alpha-activity could be observed after the relatively short lived  $\text{At}^{211}$  alpha-activity had decayed out. These results suggested that  $\text{Po}^{210}$  was formed as a decay product of a new isotope of astatine, probably by capture of an orbital electron of  $\text{At}^{210}$  which had been formed by an  $(\alpha,3n)$  reaction on bismuth.

In order to study the formation of the  $\text{Po}^{210}$  more carefully a G-M counter was constructed having an optimum X-ray counting efficiency in the region of the K X-rays of polonium. This counter was a Chicago type, having a cylindrical aluminum wall 0.25 mm thick lined with tin foil 0.06 mm thick. The counter was filled with argon plus 10 percent of alcohol to a pressure of 10 cm of mercury.

Two samples of astatine were studied with this G-M counter and with the alpha-counter. Sample A was prepared by bombarding thin bismuth with alphas of 25 Mev energy and then extracting the astatine by a vacuum distillation over to a cold platinum plate; sample B was prepared in the same way except that the bombarding alphas had an energy of 37 Mev rather than 25 Mev. Absorption in lead indicated that a gamma-ray of 1.0 Mev energy was present in sample B but was not present in Sample A, as is shown in Fig. 6. This gamma-ray was found to decay with a half-life of 8.3 hours. Absorption in aluminum showed that some 0.9 mev electrons accompanied the gamma-rays; these were in all probability conversion electrons of the 1.0 Mev gamma-rays. Absorption in platinum and tungsten revealed that both samples emitted X-rays showing the absorption properties to be expected for the K lines of polonium. The ratio of the K X-ray counting rate to the alpha counting rate was 10 to 14 times as large in sample B as in sample A. In sample A the half-life of the K X-rays was 7.5 hours; in sample B the half-life of the K X-rays was slightly more than 8 hours.  $\text{Po}^{210}$  was found in sample B but not in sample A. Clearly sample B contained a new isotope of astatine, most if not all of which decayed into  $\text{Po}^{210}$  with the omission of K X-rays and gamma-rays.

The existence of  $\text{At}^{210}$  and its decay by orbital electron capture to  $\text{Po}^{210}$  being thus established, the question arises as to whether all the  $\text{Po}^{210}$  found in our alpha bombardments was produced through the decay of  $\text{At}^{210}$  or whether some was formed directly by a  $21(\alpha,2n)$  reaction. This question could be settled in several ways. The method we chose consisted, in principle, in dividing a thin bombarded bismuth foil into two equal parts and extracting all the astatine from one part immediately after bombardment. A week later only the  $\text{Po}^{210}$  activities were left and were readily determined by alpha count-

ing each sample. If all the  $\text{Po}^{210}$  formed is a daughter of  $\text{At}^{210}$  the unextracted sample and the extracted astatine sample must each have the same activity. On the other hand if some of the  $\text{Po}^{210}$  is formed directly at bombardment then the unextracted sample must have a greater activity than the extracted astatine sample.

In practice this procedure requires enough time so that an extrapolation must be made back to the time of the middle of the bombardment. In order to make this extrapolation the procedure was repeated allowing various time intervals between the bombardment and the astatine extraction. To eliminate the effect of unequal division of the bombarded bismuth foil and variation of the extraction yield, the amount of  $\text{At}^{211}$  alpha-activity in each sample was used for normalization. The ratio of the  $\text{Po}^{210}$  resulting from the decay of the extracted astatine to the total  $\text{Po}^{210}$  formed plotted as a function of extraction time is shown in Fig. 7. The decay is seen to agree quite well with the 8.3 hour half-life found for the gamma-rays. The zero time intercept (the time of the middle of the bombardment) shows that within the experimental error all the  $\text{Po}^{210}$  was formed by the decay of the  $\text{At}^{210}$ .

Clearly the results shown in Fig. 7 are valid only if the astatine extractions are free from polonium contamination. For this reason the extraction process<sup>(11)</sup> employed here will be described briefly. When an alpha bombarded sample of bismuth on aluminum is heated in the presence of silver in an evacuated glass vessel the astatine vapor is selectively adsorbed by the silver. Careful tests have shown that after 10 minutes at  $310^\circ\text{C}$ . more than 85 percent of the astatine alpha activity was collected on the silver foil. Under the same conditions, using a bombarded bismuth sample from which all the astatine had decayed out, only 0.07 percent of the polonium alpha-activity present in the bismuth appeared on the silver foil. For this astatine separation method neither the temperature nor the heating time was very critical; however the bismuth had to be melted ( $273^\circ\text{C}$ . or more), and the polonium contamination increased slowly with increasing temperature.

If there were any appreciable alpha-branching in the decay of  $\text{At}^{210}$  as there

is in  $\text{At}^{211}$  one should see evidence of this alpha-activity and evidence of the decay product, which would be  $\text{Bi}^{206}$  with a 6.4 day half-life. Examination of extracted astatine in the 48 channel pulse analyser<sup>(12)</sup> showed no alpha-activity other than that of  $\text{At}^{211}$  and  $\text{Po}^{210}$ . If the branching ratio had been 1 part in 100 or more the resulting alpha-activity could have been observed. Examination of the astatine extracted from a thick bismuth target bombarded with 200 microampere hours of alpha particles having an energy of 37 Mev showed no evidence of 6.4 day activity. If 1 part in  $10^5$  of the  $\text{At}^{210}$  had decayed by alpha-emission the 6.4 day  $\text{Bi}^{206}$  would have been observable.

### Conclusions

The  $(d,p)$  and  $(d,n)$  reactions have recently been treated in a paper by Peaslee. In this paper he interprets our experimental material and we refer to it for details<sup>(13)</sup>. The main qualitative conclusions are that the stripping processes of the deuteron as opposed to the formation of a compound nucleus in which the whole deuteron is absorbed are mainly responsible for the observed cross sections. In the  $(d,p)$  case the stripping process is the well known Oppenheimer Philips reaction; in the  $(d,n)$  case it is an analogous reaction.

The interpretation of the  $(\alpha,2n)$  and the  $(\alpha,3n)$  reactions can be made in a very simple semiempirical way as follows.

Consider first the cross section  $\sigma_{\alpha}$  for formation of the compound nucleus. This cross section has been calculated in some typical examples by V. F. Weisskopf. In Fig. 8 the solid lines give Weisskopf's values for  $_{80}\text{Hg}^{201}$  for two values of the barrier height, 25.93 Mev and 22.47 Mev corresponding to  $r_0 = 1.3 \times 10^{-13}$  cm and  $1.5 \times 10^{-13}$  cm; the values are also given for  $_{90}\text{Th}^{232}$  for a barrier height of 28.00 Mev corresponding to  $r_0 = 1.3 \times 10^{-13}$  cm.

If we sum our  $(\alpha,2n)$  and  $(\alpha,3n)$  cross sections we find passable agreement with Weisskopf's curve. See Fig. 8. This we interpret as meaning that all other competing reactions -  $(\alpha,p)$ ,  $(\alpha,pn)$ ,  $(\alpha,\gamma)$ ,  $(\alpha,\alpha)$ , etc. - have small cross sections compared with  $(\alpha,2n)$  and  $(\alpha,3n)$  in the energy region considered. Exception to this is the  $(\alpha,n)$  reaction

which in the energy region around 20 Mev may have a cross section which, although small on an absolute scale, exceeds appreciably the  $(\alpha, 2n)$  cross section. Hence until experiments on this point are completed it will be impossible properly to fit the theoretical curve for the compound nucleus formation to our experimental data in the region near the threshold. An investigation of the  $(\alpha, n)$  cross section is in progress.

It is interesting to consider the excitation energy of the compound nucleus above its ground state. The compound nucleus  $\text{At}^{213}$  in its fundamental state would certainly be alpha radioactive. By comparison with neighboring known nuclei -  $\text{At}^{211}$ ,  $\text{AcCl}$ ,  $\text{At}^{212}$ , etc. - one would make a fair guess of a half-life of about  $5 \times 10^{-3}$  sec. and an alpha-energy of 7.5 Mev. Hence the excitation energy of the compound nucleus is approximately equal to the energy of the impinging alpha particle minus 7.5 Mev. Thus to release 2 neutrons it takes at least 21.5 Mev and to remove a 3rd neutron an additional 8.5 Mev or at least 30 Mev to remove 3 neutrons.

RLID/hw  
11-10-48

#### References

- (1) D. G. Hurst, R. Lantham, and W. B. Lewis, Proc. Roy. Soc. 174, 126 (1940).
- (2) J. M. Cork, J. Halpern, and H. Tatel, Phy. Rev. 57, 348 (1940); 57, 371 (1940).
- (3) R. S. Krishnan and E. A. Nahum, Proc. Roy. Soc. A180, 321 (1942).
- (4) J. M. Cork, Phys. Rev. 70, 563 (1946).
- (5) D. R. Corson, K. R. MacKenzie, and E. Segré, Phy. Rev. 58, 672 (1940).
- (6) A. W. Vance, Rev. Sci. Inst. 7, 489 (1936).
- (7) R. R. Wilson, Phy. Rev. 60, 749 (1941).
- (8) M. Stanley Livingston and H. A. Bethe, Rev. Mod. Phy. 9, 285 (1937).
- (9) J. H. Smith, Phy. Rev. 71, 32 (1947).
- (10) D. H. Templeton, J. J. Howland, and I. Perlman, Phy. Rev. 72, 758 (1947).
- (11) For the separation methods see Johnson, Leininger, and Segré, Chemical Properties of Astatine I. Journal of Chemical Physics, in press.
- (12) A. Ghiorso, A. H. Jaffey, H. P. Robinson and B. Weissbourd, An Alpha Pulse Analyser Apparatus (Plutonium Project Record, Vol. 14B, 17.3 (1946). (To be issued).
- (13) D. C. Peaslee, Phy. Rev. 74, 1001 (1948).

Figure Captions

- Fig. 1. Schematic diagram of the collimating tube, foil holder, and current amplifiers. This apparatus connects directly to the cyclotron tank and becomes therefore an integral part of the cyclotron vacuum system, obviating the need for any windows or separate pumps.
- Fig. 2. The percent of the  $\alpha$ -beam transmitted by the Al absorber plotted as a function of the absorber thickness. The three sets of points represent data taken before bombardment, at the middle of bombardment, and after bombardment of the bismuth foils. The straggling, given by the difference between the extrapolated range and the mean range divided by the mean range, is 1.1%.
- Fig. 3. Counts per minute of the thin U $\alpha$ -standard plotted as a function of the pulse discriminator bias voltage. The operating bias was kept constant to within 2 units.
- Fig. 4. Absolute cross section for the Bi( $\alpha$ ,2n) reaction and the Bi( $\alpha$ ,3n) reaction plotted as a function of the energy of the bombarding alphas.
- Fig. 5. Absolute cross sections for the Bi(d,p), Bi(d,n) and the Bi(d,3n) reactions plotted as a function of the energy of the bombarding deuterons.
- Fig. 6. The counting rate on a G-M counter of astatine samples plotted as a function of the thickness of lead absorber. Sample A consisted of the At extracted from a foil of Bi bombarded with alphas of 25 Mev energy; sample B consisted of the At extracted from a foil of Bi bombarded with alphas of 37 Mev. As a check of the geometry the mass absorption coefficient of a Co<sup>60</sup> $\gamma$ -standard was measured and found to be .055 cm<sup>2</sup>gm<sup>-1</sup> in Pb.
- Fig. 7. The amount of Po<sup>210</sup> formed by the decay of the extracted At<sup>210</sup>, expressed as percent of the total Po<sup>210</sup> formed, plotted as a function of the time from the middle of bombardment until the At extraction.
- Fig. 8. The cross section of the compound nucleus (At<sup>213</sup>) as a function of the energy of the bombarding nucleus. The solid lines represent the computed data of Weisskopf. The scattered points are experimental values of the sum of  $\sigma$  for Bi( $\alpha$ ,2n) and  $\sigma$  for Bi( $\alpha$ ,3n).

Table I.

Experimental Values of the Cross-Section for the  $\text{Bi}(\alpha, 2n)\text{At}^{211}$  and the  $\text{Bi}(\alpha, 3n)\text{At}^{210}$  Reactions at Various Energies of the Bombarding Alpha Particles

$\alpha$ -Energy Mev	$\sigma_{\text{At}^{211}}$			$\sigma_{\text{At}^{210}}$		
	Run I barns	Run II barns	Run III barns	Run I barns	Run II barns	Run III barns
18.8		0.000				
19.9	0.000					
20.0			0.000			
20.2		0.001				
21.2	0.01					
21.6		0.01	0.03			
22.4	0.10					
23.0		0.11				
23.1			0.16			
23.5	0.25					
24.2		0.29				
24.6	0.40		0.35			
25.4		0.45				
25.7	0.55					
26.1			0.57			
26.5		0.53				
26.7	0.67					
27.4			0.71			0.000
27.6		0.69			0.000	
27.7	0.75			0.000		
28.6	0.83		0.81	0.004		0.004
28.7		0.78			0.003	
29.6	0.90			0.013		
29.7		0.85			0.007	
29.9			0.90			0.015
30.5	0.89			0.06		
30.7		0.89			0.05	
31.0			0.91			0.10
31.4	0.86			0.17		
31.7		0.85			0.16	
32.2			0.81			0.28
32.3	0.75			0.35		
32.6		0.75			0.37	
33.1	0.62			0.53		
33.3			0.63			0.53
33.6		0.61			0.61	
34.0	0.48			0.73		
34.5			0.46			0.75
34.6		0.47			0.82	
34.8	0.39			0.93		
35.5		0.37			1.01	
35.6	0.30		0.33	1.03		0.94
36.4	0.24	0.29		1.14	1.16	
36.7			0.25			1.11
37.2	0.20	0.23		1.20	1.21	
38.0	0.17			1.24		
38.8	0.15			1.27		

Table II.

Experimental Values of the Cross-Section for the  $\text{Bi}(d,p)\text{RaE}$ , the  $\text{Bi}(d,n)\text{Po}^{210}$ , and the  $\text{Bi}(d,3n)\text{Po}^{208}$  Reactions at Various Energies of the Bombarding Deuterons.

d-Energy Mev	$\sigma_{\text{RaE}}$		$\sigma_{\text{Po}^{210}}$		$\sigma_{\text{Po}^{208}}$		d-Energy Mev	$\sigma_{\text{RaE}}$		$\sigma_{\text{Po}^{210}}$		$\sigma_{\text{Po}^{208}}$	
	Run I	Run II	Run I	Run II	Run I	Run II		Run I	Run II	Run I	Run II	Run I	Run II
	barns	barns	barns	barns	barns	barns		barns	barns	barns	barns	barns	barns
5.3		0.0002					13.7	0.110		0.033		0.02	
5.9		0.001					13.8		0.102		0.031		0.03
6.5		0.002		0.0003			14.0	0.109		0.032		0.03	
7.1		0.005		0.001			14.1		0.102		0.030		0.04
7.6		0.009		0.002			14.3	0.106		0.030		0.04	
8.1		0.016		0.004			14.5	0.104	0.098	0.031	0.030	0.05	0.05
8.6		0.026		0.007			14.8	0.101	0.095	0.031	0.031	0.07	0.07
8.7	0.030		0.006				15.1	0.096	0.093	0.032	0.031	0.10	0.10
9.0	0.040	0.037	0.009	0.010			15.3	0.097		0.030		0.12	
9.4	0.051	0.051	0.011	0.013			15.4		0.088		0.030		0.14
9.7	0.062		0.014				15.55	0.094		0.032		0.15	
9.8		0.064		0.017			15.7		0.086		0.031		0.17
10.1	0.073		0.016				15.8	0.091		0.030		0.19	
10.2		0.076		0.020			16.0		0.082		0.029		0.23
10.4	0.082		0.019				16.05	0.089		0.030		0.24	
10.6		0.084		0.023			16.3	0.084	0.081	0.030	0.030	0.27	0.27
10.7	0.091		0.023				16.5	0.084		0.031		0.31	
11.0	0.099	0.095	0.026	0.026			16.6		0.078		0.030		0.33
11.3	0.104		0.028				16.75	0.084		0.031		0.36	
11.4		0.100		0.028			16.9		0.077		0.030		0.38
11.6	0.108		0.029				17.0	0.082		0.031		0.41	
11.8		0.105		0.029			17.1		0.073		0.032		0.43
11.9	0.111		0.030				17.2	0.079		0.031		0.46	
12.2	0.112	0.107	0.030	0.031			17.4	0.074	0.071	0.031	0.031	0.51	0.50
12.5	0.114	0.109	0.030	0.031		0.01	17.7	0.075	0.070	0.030	0.032	0.55	0.53
12.8	0.114		0.031				17.9	0.074		0.032		0.59	
12.9		0.108		0.029		0.02	18.0		0.067		0.032		0.59
13.1	0.113		0.030		0.01		18.1	0.072		0.030		0.64	
13.2		0.108		0.031		0.02	18.3	0.073	0.067	0.032	0.029	0.66	0.66
13.3	0.113		0.030		0.02		18.5	0.070	0.066	0.032	0.031	0.71	0.69
13.5	0.112	0.107	0.031	0.031	0.02	0.02	18.7	0.068		0.030		0.75	

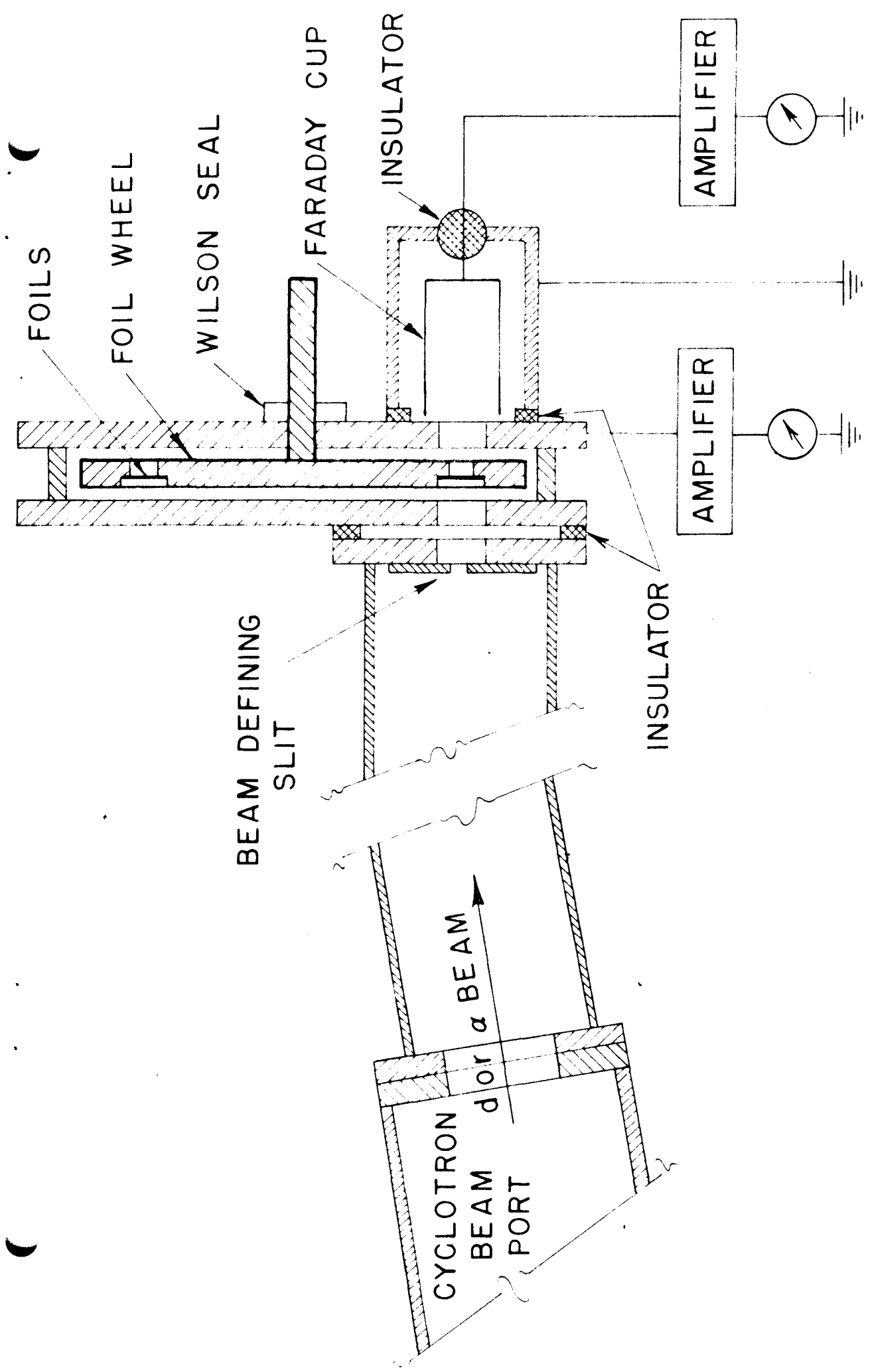


FIG. 1

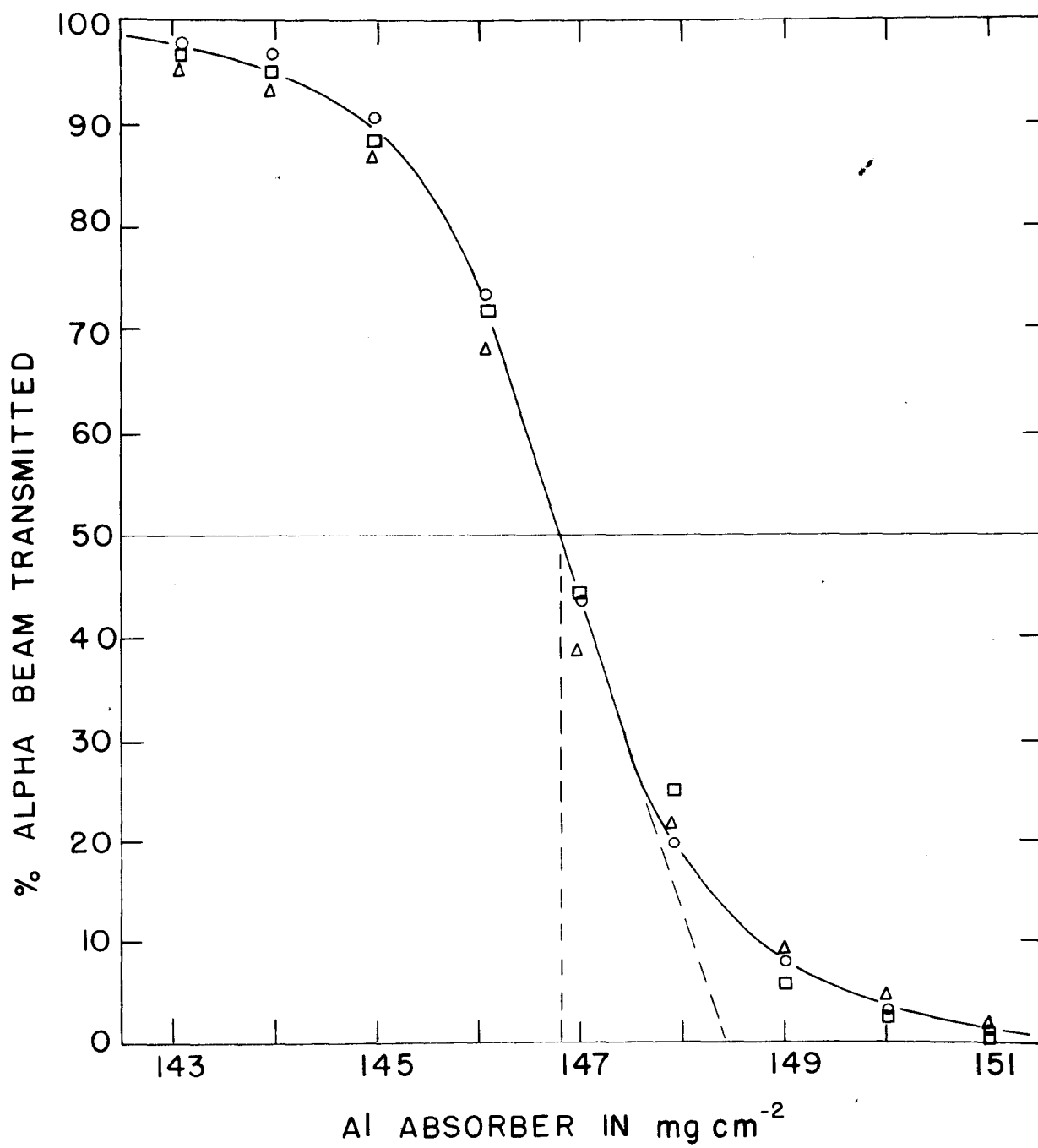


Fig 2

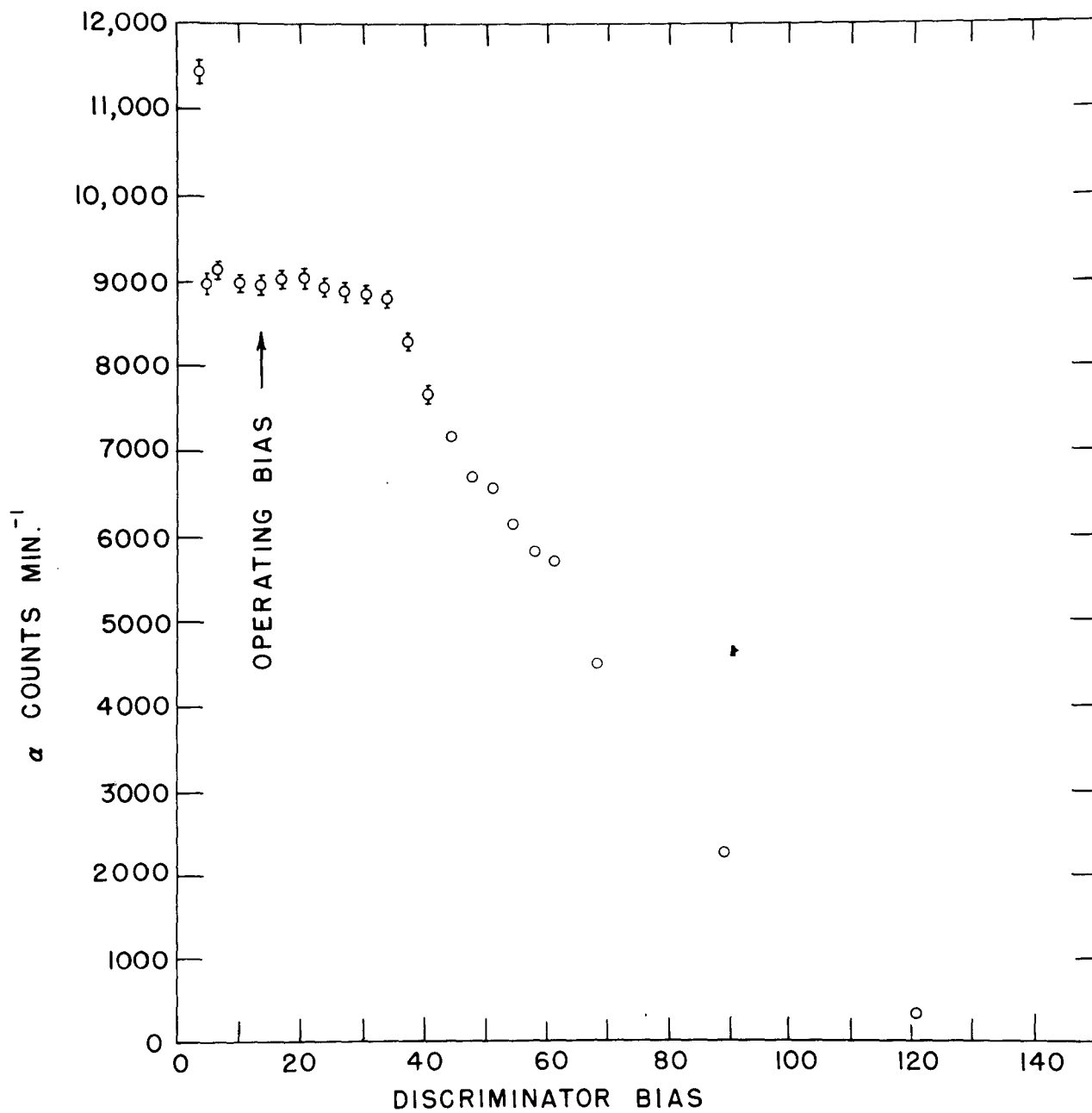


FIG. 3

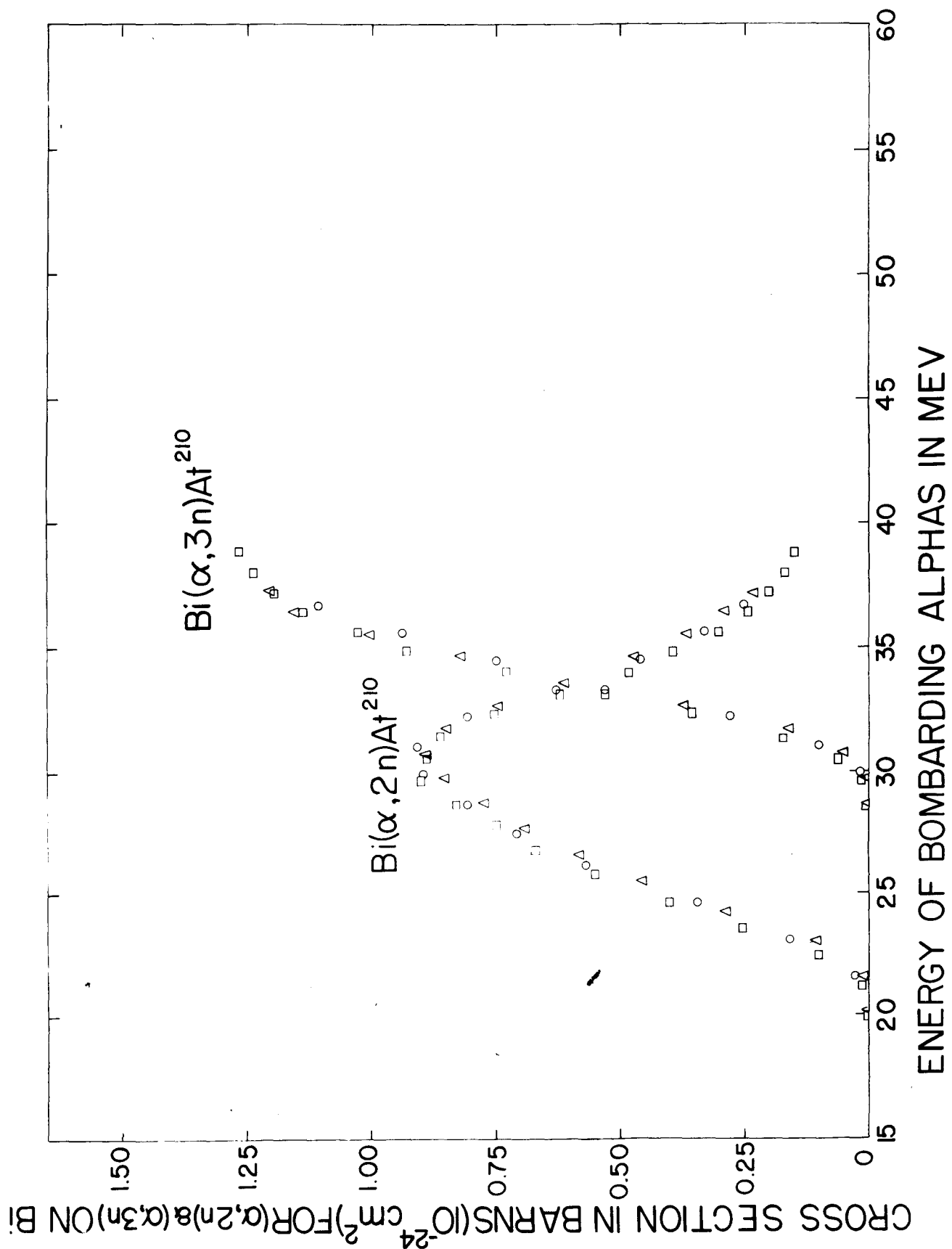


FIG. 4

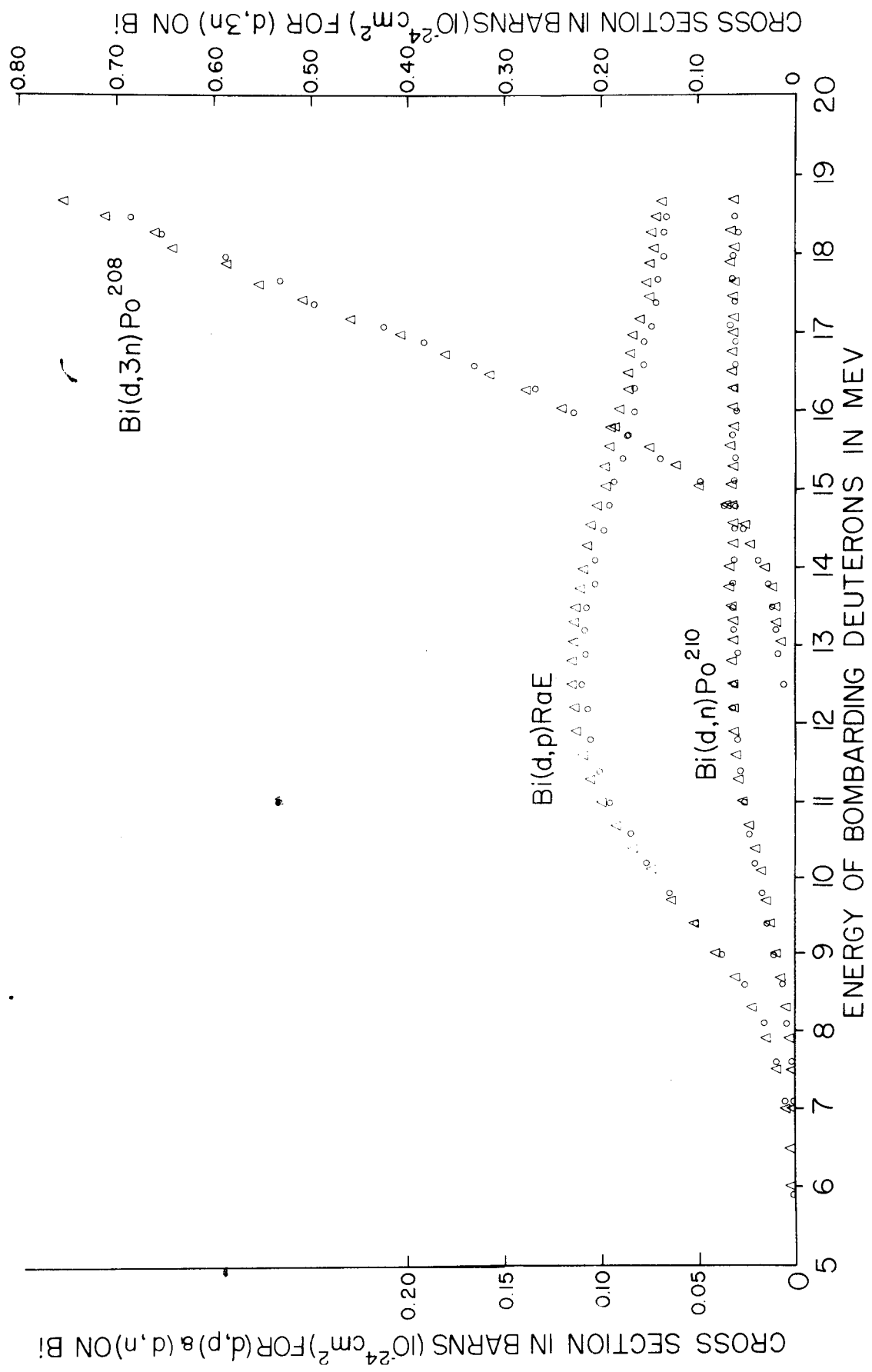


FIG. 5

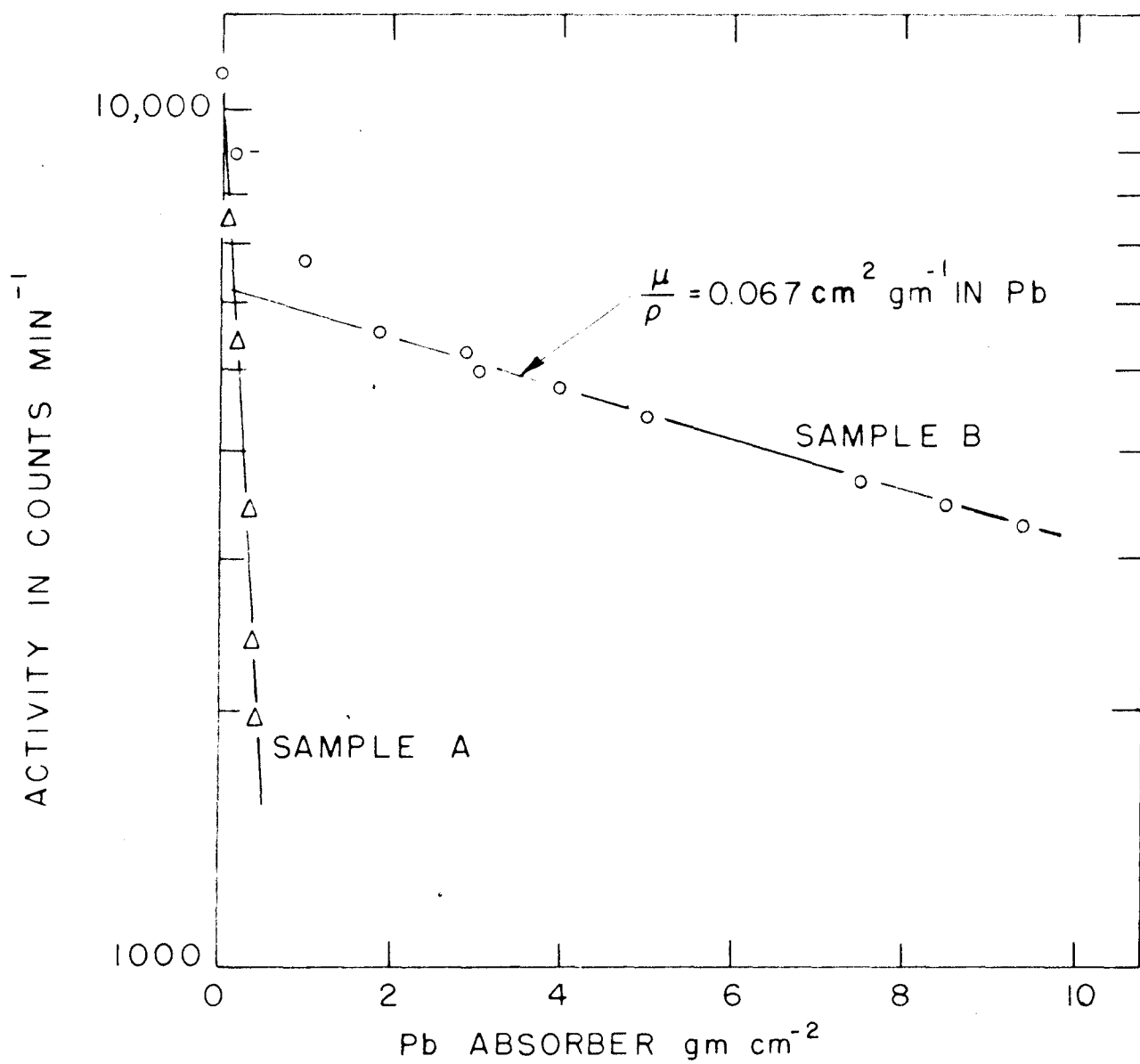
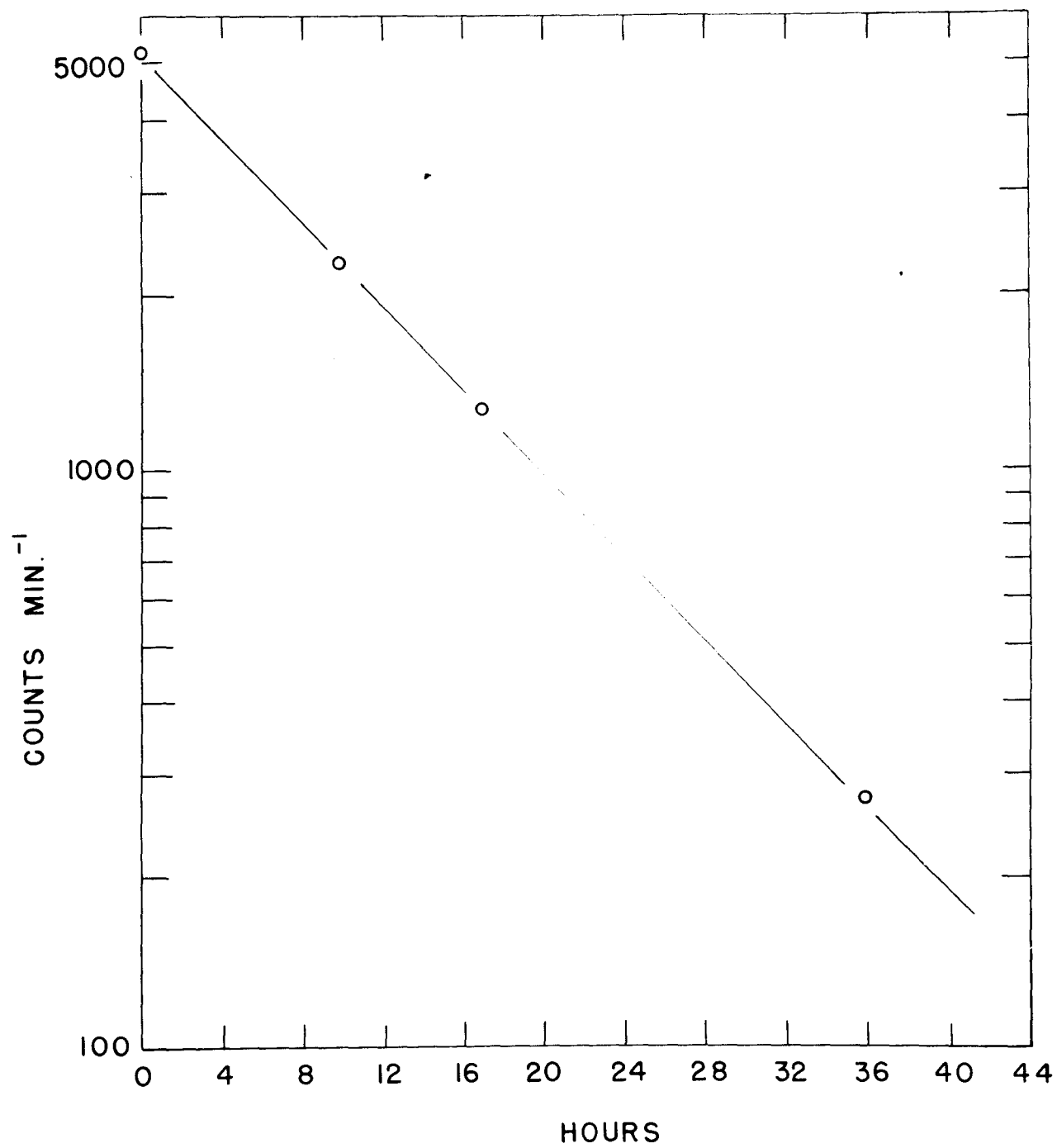
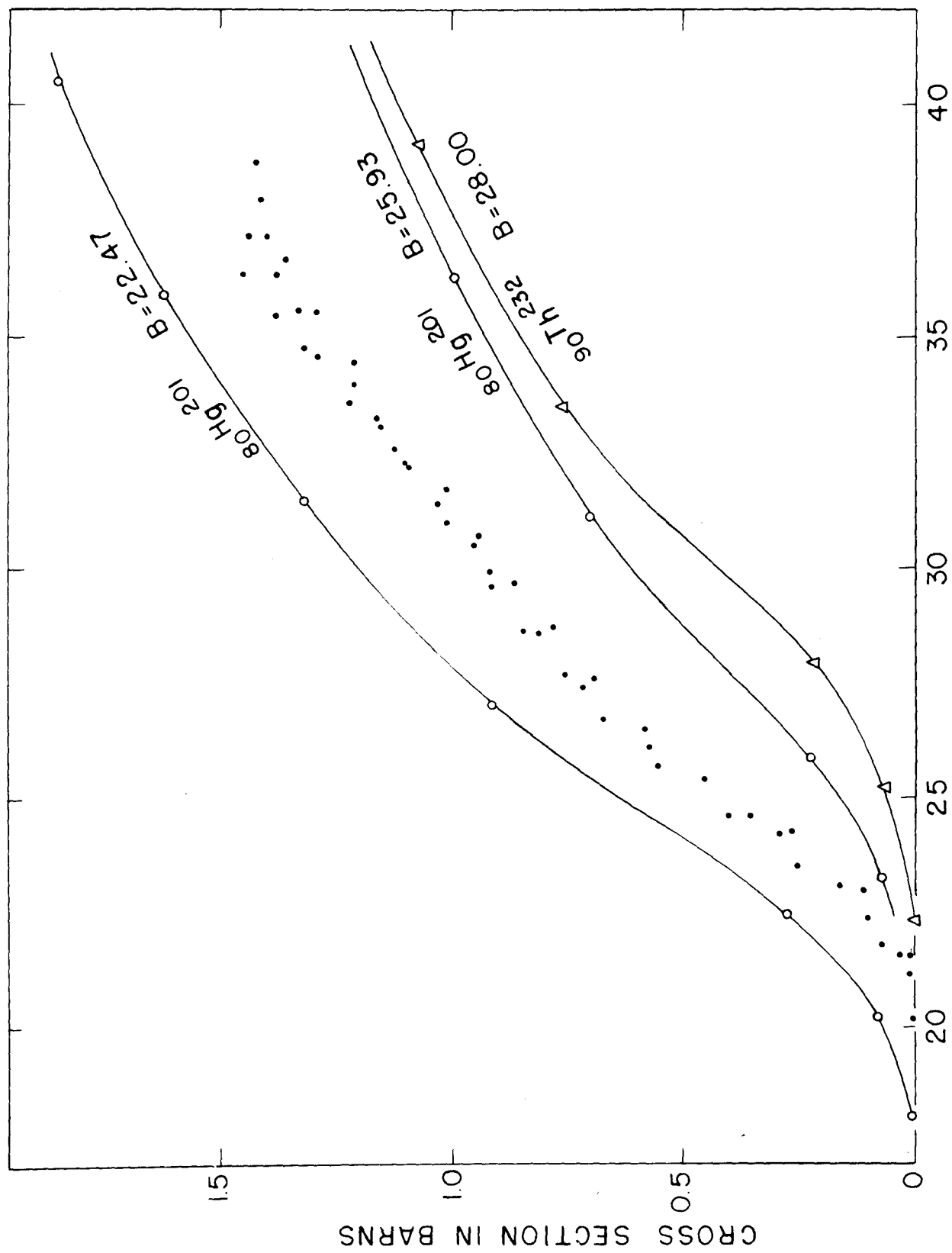


FIG 6



• FIG. 7



ENERGY OF BOMBARDING ALPHAS IN MEV

FIG 8